

## A Suspended Low Power Gas Sensor With In-Plane Heater

Palash Kumar Basu, Samatha Benedict, Sangeeth Kallat, and Navakanta Bhat, *Senior Member, IEEE*

**Abstract**—An ultralow power suspended gas sensor with in-plane heater and nano gap sensor electrodes is presented. The heater and sensing electrodes, separated by  $1\text{-}\mu\text{m}$  air gap, are processed using single lithography step with standard micro-fabrication techniques. Controlled electromigration is used to create a nanogap in the middle of the sensing electrode. The sol-gel grown ZnO is dispensed using a picoliter dispenser to bridge the nanogap electrode, created by electromigration, to get required metal oxide film as a sensing element. The gap between the electrode and heater is optimized by electrothermal simulation to obtain desired temperature profile on ZnO. The resulting device exhibits excellent sensing performance for hydrogen ( $\sim 86\%$  at 20 ppm) at 0.5 mW. A detailed characterization was carried out to analyze the performance of the device. This unique, in-plane structure is superior compared with the conventional out of plane structure in terms of the power efficiency and ease of processing. [2016-0162]

**Index Terms**—Low power  $\text{H}_2$  sensor, suspended in-plane structure, nano gap.

### I. INTRODUCTION

SEMICONDUCTING metal oxides like  $\text{SnO}_2$ ,  $\text{ZnO}$ , and  $\text{TiO}_2$  have long been used for detecting poisonous (CO) and inflammable gases ( $\text{CH}_4$ ,  $\text{H}_2$  etc.) by measuring the change in their electrical conductivity [1]–[3]. These oxides are also attractive due to their easy availability and low cost of production. Conventional thick film metal oxide gas sensors on alumina substrate or thin film MEMS (Microelectromechanical System) based gas sensors on Si substrate are commonly used for sensing gases. However, they suffer from two limitations, viz. (a) their relatively high operating temperature ( $\geq 300^\circ\text{C}$ ) and (b) large power dissipation (20mW–300 mW) [4], [5]. Usually, for sensing gases, the temperature of the sensing oxide layer should be raised to a high value to enable redox reactions. So a large amount of power is required and hence, microheater is the major constraint for low power gas sensor applications. Microheater optimization is becoming increasingly important in gas sensing applications where low power designs and long life of devices are required. Typical power consumption of microheater with active area of  $100\mu\text{m}^2$  is in the range of about 100mW. The thermal mass of the heater is typically reduced through bulk micro-machining process involving Si wafer etching using KOH or DRIE process, which can also affect the yield. In addition most of the MEMS gas sensors use heater and sensing electrodes in two different planes [6] necessitating

Manuscript received July 14, 2016; revised November 24, 2016; accepted December 2, 2016. Date of publication December 26, 2016; date of current version February 1, 2017. This work was supported in part by MCIT, in part by DAE, and in part by NPMAS. The work of P. K. Basu was supported by the Indian Institute of Science, Bangalore, under the Centenary Postdoctoral Fellowship. Subject Editor J.-B. Yoon.

P. K. Basu was with the Centre for Nano Science and Engineering, Indian Institute of Science at Bangalore, Bangalore 560012, India. He is now with the Department of Avionics, Indian Institute of Space Science and Technology at Thiruvananthapuram, Thiruvananthapuram 695547, India.

S. Benedict, S. Kallat, and N. Bhat are with the Centre for Nano Science and Engineering, Indian Institute of Science at Bangalore, Bangalore, India (e-mail: navakant@ece.iisc.ernet.in).

Color versions of one or more of the figures in this paper are available online at <http://ieeexplore.ieee.org>.

Digital Object Identifier 10.1109/JMEMS.2016.2636333

1057-7157 © 2016 IEEE. Personal use is permitted, but republication/redistribution requires IEEE permission.

See [http://www.ieee.org/publications\\_standards/publications/rights/index.html](http://www.ieee.org/publications_standards/publications/rights/index.html) for more information.

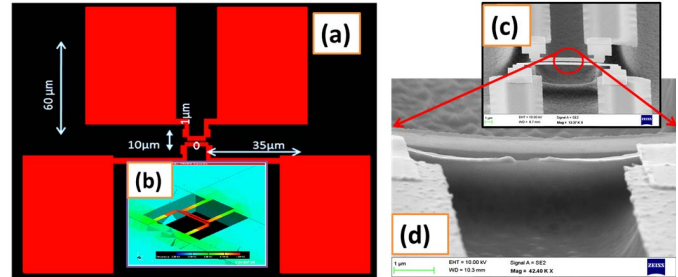


Fig. 1. The (a) schematic of the in-plane sensor. (b) Steady state electrothermal simulation at an applied voltage of 0.5V. (c, d) SEM image of the fabricated device.

two separate lithography steps- one for the heater and second for the sensing electrodes.

Detection of  $\text{H}_2$  is one of the important requirements as it is a hazardous, odourless and highly inflammable gas. It is necessary to detect its leakage at low ppm levels. There are plenty of reports available on Hydrogen sensors [7]–[9]. These sensors would typically utilize complex fabrication processes and operate with a power consumption of more than 10mW. In this report we demonstrate suspended in-plane hydrogen sensor, containing the heater and nanogap electrode. The process flow is very simple and the nano gap sensor electrode is created by standard electromigration technique to enhance the performance of hydrogen sensing. The nano gap is bridged using solution processed ZnO as the sensing element. The power consumption of the heater is very low ( $<0.5\text{mW}$ ) as compared to the reported literature.

### II. MATERIALS AND METHODS

Fig.1 shows the schematic of the in-plane heater. The active area consists of two suspended  $1\mu\text{m}$  wide Pt metal beams. The small beam is the heater and the long beam is the sensing electrode. The separation between the two beams is  $1\mu\text{m}$ . The electrothermal simulation carried out using Coventorware indicates that the temperature is maximum at the middle suspended portion and gradually decreases on either sides, reaching substantially low values at the anchor portion due to large thermal mass. However, it can be observed the voltage applied to one of the beam (heater), generates heat due to joule heating, which in turns couples to the neighbouring beam (sensing beam) very efficiently, through convection.

The suspended in-plane structures were realized on oxidized Silicon substrates, by sputter depositing of Pt (100nm) followed by a single step reactive ion etching using  $\text{CF}_4$  chemistry. The detailed fabrication process flow is shown in Fig. 2.

### III. RESULTS AND DISCUSSIONS

The temperature of the microheater and sensor electrode is estimated from the TCR (temperature coefficient of resistance) value which is extracted from Resistance–Temperature plot, shown

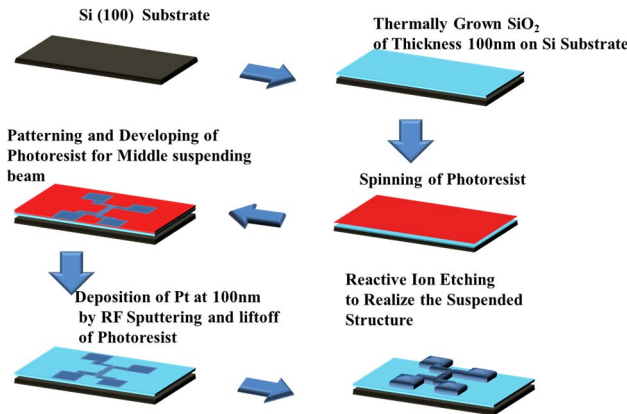


Fig. 2. The process flow of the fabricated device.

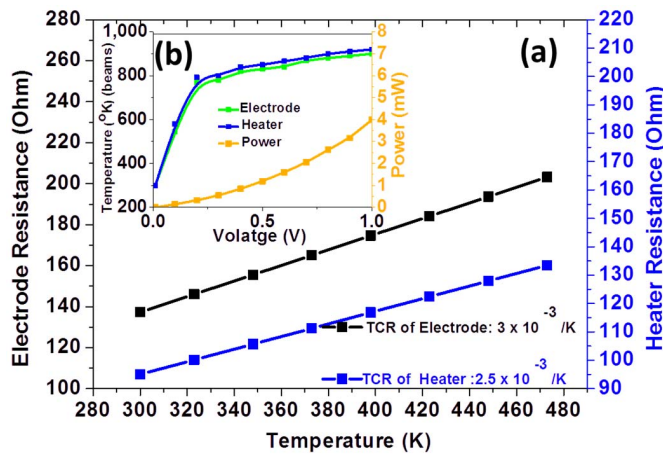


Fig. 3. The change of resistance (heater and sensor electrode) with temperature (a). The TCR (temperature coefficient of resistance) value is calculated from the slope. The temperature generated across the beams (b) is calculated using this TCR value.

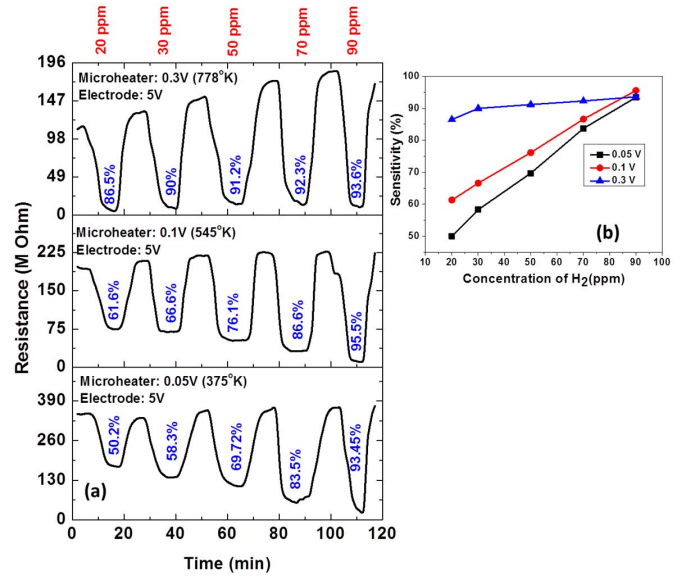
in Fig. 3(a). It is known that the dependence of the specific resistance on temperature can be expressed by the following formula [11], [12]

$$R_T = R_{T_0} [1 + \alpha (T - T_0)]$$

Where  $R_T$  and  $R_{T_0}$  are the heater resistances at temperatures  $T$  and  $T_0$ , respectively, and  $\alpha$  is the temperature coefficient of the resistance. The temperature coefficient of resistance (TCR) value of the in-plane microheater and electrode are  $2.5 \times 10^{-3}/K$  and  $3 \times 10^{-3}/K$  which agree well with the other reported literature [12].

The estimated temperature, from the change of resistance due to joule heating in the microheater, is calculated from the measured TCR values and is shown in Fig. 3b. In order to estimate the temperature rise in the neighbouring electrode beam, we measure its resistance at very low voltage (20mV) so that there is negligible heating due to this applied voltage. From Fig. 3b, we also note that, the heater temperature reaches to about 800K at an applied voltage of 0.3V, with power consumption of about 0.5mW

The nanogap is created in sensing electrode of the gas sensor by standard electromigration technique. By applying large electric field, the momentum of the moving electrons is transferred to the metal ions in the lattice sites, which results in the gradual movement of the ions and finally a nanogap is created [11], [12]. Fig. 1d clearly shows the creation of nanogap at high voltage (0.7 V). The current initially increases up to 0.7V and after that, the current suddenly drops to


 Fig. 4. (a) The transient response curve of in-plane sensor at different heater voltages. (b) Sensitivity versus  $H_2$  concentrations.

zero, due to electromigration induced nanogap ( $\sim 400$ nm). Finally, the ZnO, the active material for  $H_2$  sensor, was prepared by Sol-Gel technique. 0.45M zinc acetate dehydrate [ $Zn(CH_3COO)_2 \cdot 2H_2O$ ] (98%) was used as the chemical precursor.

The acetate was mixed with isopropanol and stirred well at room temperature. When the solution turned milky, diethanolamine (DEA) was added slowly to yield a clear transparent homogeneous solution. After aging for 24h, the solution was dispensed by Pico litre dispenser to bridge the nanogap electrode and annealed at  $500^\circ C$  for 1 hr. It should be noted that the creation of heater and sensing electrode along with sensing material, in the same plane, results in an efficient fabrication process flow. A single lithography step is adequate, as opposed to two lithography steps for the conventional out of plane heater. The sensing properties of the in-plane beams are characterized at different microheater voltages, with a volumetric gas calibration system using gases with purity levels benchmarked with NIST (National Institute of Standards and Technology) traceable standards. Prior to the experiments, the sample is purged with synthetic air for several hours until the current is stabilized. The transient response curves (Fig. 4a) of the in-plane sensors using dispensed ZnO were studied with different concentrations of Hydrogen (20ppm, 30ppm, 50ppm, 70ppm and 90 ppm) in synthetic air at different microheater voltages (0.05V, 0.1V and 0.3V). The sensitivity was calculated using the relation,  $S = \frac{\Delta R}{R_0} \times 100$ . At an elevated temperature, oxygen from the air is adsorbed onto the surface of the ZnO and forms negatively charged surface ions by gaining electrons from the ZnO, yielding a high resistance surface. These electrons come back to the ZnO surface again during the interaction of Hydrogen and adsorbed oxygen, resulting in a lower resistance. The sensitivity for given  $H_2$  concentrations, increases with increasing heater voltage, as shown in Fig 4b. This is due to the increase in sensor film temperature with increase in heater voltage. The higher sensor temperature is expected to result in more efficient redox reactions, thus enhancing the sensitivity. At an applied heater voltage of 0.3V, the sensor consumes 0.5mW power and provides a sensitivity of 86% for 20ppm  $H_2$  gas. Even with an applied heater voltage of 0.05V, the sensor operates at about 375K, and gives 50% sensitivity for 20ppm  $H_2$  gas, while consuming  $50\mu W$  power. From the transient

response cycles the response time and recovery time are in the range of 2 to 3 minutes. The response and recovery time can be further improved by functionalizing the metal oxide with some catalyst metals [30].

It is further noticed that sensitivity at 0.3V is lower than those at other voltages when the gas concentration is 90 ppm. This suggests an optimum temperature for better sensitivity, and higher temperature does not always give better sensitivity. This can be explained by the adsorption –desorption of gases on metal oxide. In this case the cause of sensitivity change upon exposure is due to H<sub>2</sub> adsorption on the active sites of the metal oxide and subsequent lowering of the resistance. The adsorption – desorption phenomena can be explained by Langmuir isotherm which defines the dependence of the surface coverage of an adsorbed species on the pressure of the gas above the surface at a particular temperature. These include two important parameters i.e. the temperature of the system and the pressure of the gas above the surface. In general these two factors exert opposite effects on the concentration of the adsorbed species: the surface coverage may be increased by increasing the gas pressure but will be reduced if the temperature is raised. The optimum conditions of maximum adsorption occur at a particular temperature and pressure. In this case the temperature was varied from 375K to 778K and the response peaks at 545K for 90 ppm H<sub>2</sub>. At higher temperatures, desorption of hydrogen from the surface dominates and thus the response decreases.

In conclusion, we demonstrate new device architecture with in-plane microheater, for low power gas sensor application. The suspended microheater temperature reaches to about 800K at an applied voltage of 0.3V, with power consumption of about 0.5mW. The sensor has been validated for H<sub>2</sub> gas sensing using solution dispensed ZnO film to bridge the nano-gap in sensor electrode created using electromigration. The sensor provides a response of 86% at 20ppm H<sub>2</sub> concentration. This device architecture can also be extended for other gases using different sensing materials.

## REFERENCES

- [1] W. Li *et al.*, “New model for a Pd-doped SnO<sub>2</sub>-based CO gas sensor and catalyst studied by online in-situ X-ray photoelectron spectroscopy,” *J. Phys. Chem. C*, vol. 115, no. 43, pp. 21258–21263, Oct. 2011.
- [2] Y. Zenga *et al.*, “Development of microstructure CO sensor based on hierarchically porous ZnO nanosheet thin films,” *Sens. Actuator B, Chem.*, vol. 173, pp. 897–902, Oct. 2012.
- [3] H. G. Moon *et al.*, “Highly sensitive CO sensors based on cross-linked TiO<sub>2</sub> hollow hemispheres,” *Sens. Actuator B, Chem.*, vol. 149, no. 1, pp. 116–121, Aug. 2010.
- [4] A. Forta *et al.*, “Metal-oxide nanowire sensors for CO detection: Characterization and modeling,” *Sens. Actuator B, Chem.*, vol. 148, no. 1, pp. 283–291, Jun. 2010.
- [5] L. Xu, Y. Wang, H. Zhou, Y. Liu, T. Li, and Y. Wang, “Design, fabrication, and characterization of a high-heating-efficiency 3-D microheater for catalytic gas sensors,” *J. Microelectromech. Syst.*, vol. 21, no. 6, pp. 1402–1410, Dec. 2012.
- [6] J. Courbat, M. Canonica, D. Teyssieux, D. Briand, and N. F. D. Rooij, “Design and fabrication of micro-hotplates made on a polyimide foil: Electrothermal simulation and characterization to achieve power consumption in the low mW range,” *J. Micromech. Microeng.*, vol. 21, no. 1, p. 015014, Dec. 2010.
- [7] T. Hübert, L. Boon-Brett, G. Black, and U. Banach, “Hydrogen sensors—A review,” *Sens. Actuator B, Chem.*, vol. 157, no. 2, pp. 329–352, Oct. 2011.
- [8] F. Yang, S.-C. Kung, M. Cheng, J. C. Hemminger, and R. M. Penner, “Smaller is faster and more sensitive: The effect of wire size on the detection of hydrogen by single palladium nanowires,” *ACS Nano*, vol. 4, no. 9, pp. 5233–5244, Aug. 2010.
- [9] F. Yang, K. C. Donovan, S.-C. Kung, and R. M. Penner, “The surface scattering-based detection of hydrogen in air using a platinum nanowire,” *Nano Lett.*, vol. 12, no. 6, pp. 2924–2930, May 2012.
- [10] S. Fardindoost, A. I. Zad, F. Rahimi, and R. Ghasempour, “Pd doped WO<sub>3</sub> films prepared by sol–gel process for hydrogen sensing,” *Int. J. Hydrogen Energy*, vol. 35, no. 2, pp. 854–860, Jan. 2010.
- [11] Y. Zhai, C. Cai, J. Huang, H. Liu, S. Zhou, and W. Liu, “Study on the resistance characteristic of Pt thin film,” in *Proc. 18th Int. Vac. Congr. (IVC)*, vol. 32, Jun. 2012, pp. 772–778.
- [12] G. Esen and M. S. Fuhrera, “Temperature control of electromigration to form gold nanogap junctions,” *Appl. Phys. Lett.*, vol. 87, no. 26, p. 263101, Dec. 2005.